

Separation and Utilization of Tc and Other Rare Metal Fission Products by an Extended Aqueous Reprocessing

Masaki Ozawa,^{*,a,b} Shinichi Koyama,^a Tatsuya Suzuki,^b and Yasuhiko Fujii^b

^aO-arai Engineering Center, Japan Nuclear Cycle Development Institute, Oarai-machi, Higahibaraki-gun, Ibaraki 311-1393, Japan

^bResearch Laboratory for Nuclear Reactors, Tokyo Institute of Technology, O-okayama, Meguro-ku, Tokyo, Japan

Received: July 31, 2005; In Final Form: September 30, 2005

A novel reprocessing system with recovery of actinides, long-lived fission products (LLFP) and valuable rare metal fission products (RMFP) has been proposed. This process is based on ion exchange (IX) and catalytic electrolytic extraction (CEE). The pre-filtration step using tertiary pyridine-type anion-exchange resin is set prior to the main actinide recovery steps in this system. The perfect isolation of platinum group elements (Pt-G) such as 106Ru from fuel dissolver solution was successfully demonstrated for irradiated mixed oxide (MOX) fuel. The CEE method, being set as a post-pre-filtration process, was applicable to separation of RMFP including TcO_4^- and ReO_4^- by selective and accelerative deposition with Pd^{2+} as a catalyst. Quaternary Pd-Ru-Rh-Re deposited Pt electrodes showed the highest cathodic current. The catalytic ability is about twice superior to that of the base Pt electrode when used for artificial sea water as well as alkaline solution.

The recovery and separation of actinides and RMFP by a multi-functional reprocessing system consisting of IX and CEE will minimize the quantity and improve the quality of high level liquid waste (HLLW). The recovered RMFP will be used as a "FP-catalyst" for hydrogen production in water electrolysis.

1. Introduction

In order to optimize the radioactive waste treatment in the nuclear fuel cycle, partitioning and transmutation (i.e. P&T) of actinides (An) and fission products (FP) have been considered. Actinides are α radioactive, and their half-lives are long; e.g. 2.4×10^4 , 4.3×10^2 and 2.1×10^6 years for ^{239}Pu , ^{241}Am and ^{237}Np , respectively. Among FPs concerned, Tc, Pd, Se and Te are long-lived fission products (LLFP), and Ru, Rh, Pd, Tc, Se and Te are precious and rare metal fission products (RMFP). The half-life of ^{99}Tc is as long as 2.1×10^5 years. By considering its fate, utilization with and without transmutation ($^{99}Tc(n,\gamma)^{100}Tc \rightarrow \beta^- \rightarrow ^{100}Ru(\text{stable})$) are pictured in the future. Typical amounts of FP estimated by calculations with the ORIGEN-II code are shown in Table 1. Amounts of RMFP generated are proportional to burnup of the fuel, and spent mixed oxide (MOX) fuel, highly irradiated in fast reactor (burnup: 150 GWd/t, cooling time: 4 years), will contain more than 30 kg of RMFP per metric ton.

TABLE 1: Typical Amount of RMFP Per Ton of Fast-reactor Spent Fuel

Pure metal	Ru	Rh	Pd	Tc	Te	Se	Note
Amount (kg/HMt)	12.5	3.6	11.1	3.3	2.7	0.2	FBR-SF; 150 GWd/t, Cooled 4 years.

It is, therefore, indispensable to establish effective separation methods and a way of utilization as the concept of P&T,U (Partitioning, Transmutation and Utilization) by using innovative technologies.^{1,2} Thereby, the HLLW containing non- α , non-LLFP and non-RMFP nuclides would be preferably produced for a non-deep disposal.

The current fuel reprocessing system cannot respond to such

*Corresponding author. E-mail: ozawa.masaki@jaea.go.jp. FAX: +81-29-267-1676.

delicate processes as recovery and separation of LLFP and RMFP. We propose a new reprocessing system based on ion exchange (IX) and catalytic electrolytic extraction (CEE) methods. The state-of-the-arts of separation technology on RMFP and minor actinides (MA) from spent fuel by the IX method and utilization technology of RMFP (including Tc) and Re (as hydrogen generation catalysts) by the CEE method are described.

2. Novel Reprocessing System Provided with Separation Function of LLFP and RMFP

An innovative reprocessing system is newly proposed. A schematic diagram of the process is shown in Figure 1. The process is based on IX chromatography using pyridine resin.

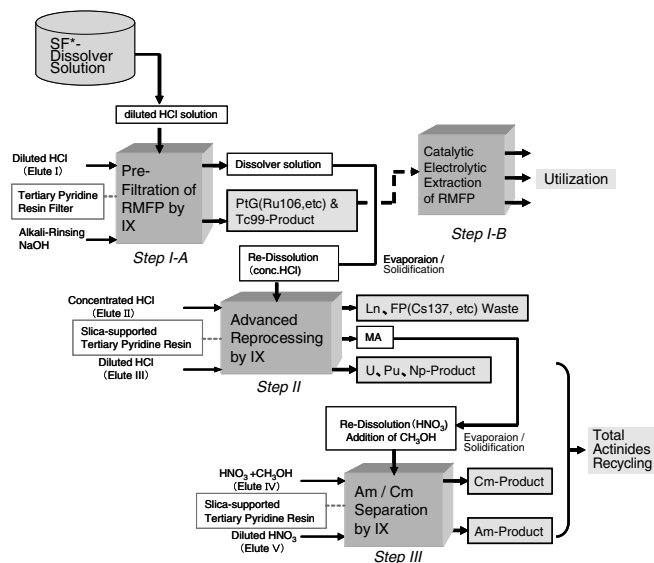


Figure 1. Reprocessing flow sheet provided with multi-functional separation ability.

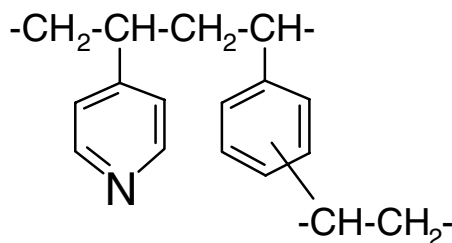


Figure 2. Chemical form of tertiary pyridine-type anion exchange resin.

Tertiary pyridine resin has functions of a weakly basic anion exchanger and a soft donor extractant. As shown in Figure 1, the reprocessing system mainly consists of three processes; the first step (Step I-A) consists of a pre-filtration process prior to main reprocessing of Step II and a recovery process of RMFP by CEE (Step I-B). Step II is the main process for separation of spent fuel, i.e. spent fuel is separated into 3 groups such as FPs with Ln (III), MA (III), and Pu with U, Np. The fraction of FPs with Ln(III) will be HLLW. The third step (Step III) is a mutual separation process of MA(III) to Am and Cm products.

On Step I-A, technetium and Pt-G elements are expected to adsorb on the gelled tertiary pyridine resin in the diluted hydrochloric acid medium referring to the basic adsorption property on anion exchange resin. The adsorbed elements are rinsed out by alkaline elution from the resin. Technetium and Pt-G elements in this effluent are recovered again on an electrode by CEE.

On Step II, the column packed with a high-porous type of tertiary pyridine resin embedded in silica beads is used for hydrochloric acid-based reprocessing. The resin was produced by Research Laboratory for Nuclear Reactors, Tokyo Institute of Technology.³⁻⁵ The chemical structure of this resin is presented in Figure 2. The resin has high radiation resistance in hydrochloric acid solution. The average diameter of the resin is 60 μm . The total exchange capacity is 1.94 meq/g (dry) in Cl⁻ form and the cross-linkage is 20%. While multivalent U(VI), Np(VI) and Pu(IV) are strongly adsorbed on anion exchange resin in highly concentrated hydrochloric acid solution,⁶ the distribution of trivalent MA(III) and Ln(III) are lower than the multivalent Ans in such a medium. Moreover, the distribution coefficient of Ce(III) was about 4 times lower than those of Am(III) in a pure hydrochloric acid. Therefore, groups of Ln(III) with other FPs like Cs and Sr, trivalent MA(III) and multivalent U(VI), Np(VI) and Pu(IV) are individually separated in this order.

The mutual separation of Am and Cm at Step III is already confirmed by trace experiments.⁴ In this process, the same resin as on Step II was used, while nitric acid solution was used instead of hydrochloric acid solution.

3. Separation and Recovery of RMFP

Separation of RMFP by tertiary pyridine resin (Step I-A). Mixed oxide (MOX) fuel, 21.0-wt% Pu in 18.0-wt% enriched uranium, was irradiated from the 16th to 35th cycle at the 3rd row in the experimental fast reactor JOYO. The effective full power days were 1019.33, and the peak burnup was 143.8 GWd/t. A total of 1560 days have passed from the reactor shut down to analysis.

A chopped irradiated fuel pin was transported to Alpha-Gamma Facility (AGF) of the Japan Nuclear Cycle Development Institute. The irradiated fuel was further sliced into pieces of 5 mm in length at AGF.

The sliced specimen was then placed in a flask mounted with reflux condenser, and dissolved in 28 mL of 8 mol/dm³ nitric acid solution by heating for 6 h at boiling temperature.

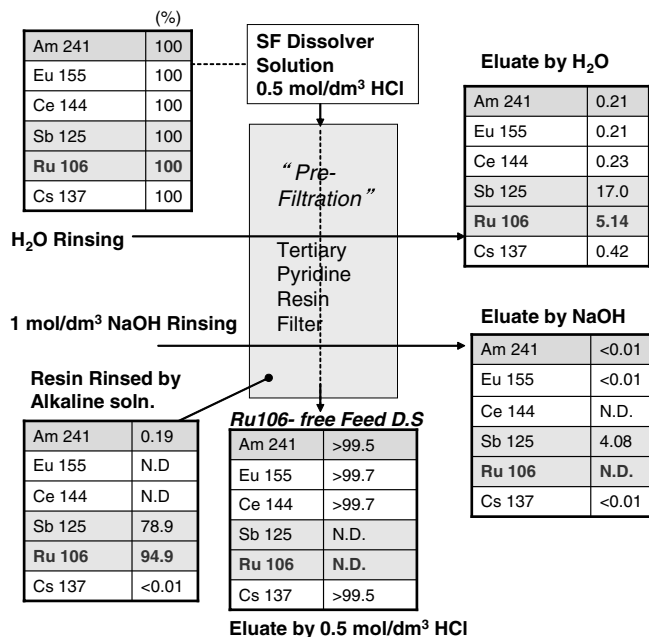


Figure 3. Material balance of ¹⁰⁶Ru and Other FP on pre-filtration (STEP I-A).

After several drops of concentrated hydrofluoric acid were added, the solution was again heated for 6 h in order to minimize amounts of insoluble residue. The weight of dissolved fuel was estimated to be 1.27 g.

The fundamental flow sheet is based on a concept shown in Figure 1. The separation on Step I-A was employed to remove RMFP (¹⁰⁶Ru, ⁹⁹Tc, etc.). On this step, gamma spectrometry was applied to identify gamma nuclides like ¹⁰⁶Ru, ¹²⁵Sb, ¹⁴⁴Ce, ¹⁵⁵Eu, ²⁴¹Am and so on.

A 0.1 mL aliquot of the dissolved spent fuel solution was diluted by adding 50 mL of pure water. The sample solution was heated and dried, and was dissolved again in 3 mL of 0.5 mol/dm³ hydrochloric acid. The resulted hydrochloric dissolver solution was loaded onto resin (8 mL column volume). Tertiary pyridine resin of a non-support type was used as pre-filter anion exchange resin. After sample loading, the column was fed with 4 column volumes of 0.5 mol/dm³ hydrochloric acid solution. The resin was rinsed by pure water of 4 column volumes. Then, 1 mL of resin was taken from the column and rinsed again by pure water. After the rinse, the rinsing water and resin were encapsulated in a plastic vial. Furthermore, 3 column volumes of 1 mol/dm³ sodium hydroxide solution were fed to the resin. After the alkali rinse, the resin and eluted sodium hydroxide solution were analyzed by γ -ray spectrometry to confirm the adsorbed nuclides.

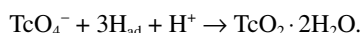
Strong γ -ray peaks of ¹⁰⁶Ru and ¹²⁵Sb were observed in the resin rinsed by pure water after anion-exchange. Other nuclides, such as ²⁴¹Am and ¹³⁷Cs were scarce. Figure 3 shows the material balance of main nuclides before and after the pre-filtration. A weight ratio of nuclide was assumed 100% at the inlet. Ruthenium-106 and ¹²⁵Sb were not detected in the eluate by elution with 0.5 mol/dm³ hydrochloric acid solution. While other nuclides, ²⁴¹Am, ¹⁵⁵Eu and ¹³⁷Cs, were scarcely detected in the outlet of rinsing water and alkaline solution, the amounts of each nuclide were less than 0.5%. It is concluded that ¹⁰⁶Ru and ¹²⁵Sb can be isolated perfectly from the spent fuel and the α contamination is very small. Noticeable FP (¹⁰⁶Ru and ¹²⁵Sb)-free dissolver solution is preferable to increase the decontamination factor in the whole reprocessing process.

Since the tertiary pyridine is a soft donor ligand and the ions of Pt-G elements are soft acid, they are strongly bonded by coordination. Technetium (⁹⁹Tc) was not detected by γ -spectrometry. Although absorption of Tc(VII), Ru(IV) and Pd(II) on Dowex 1 resin in hydrochloric acid decreases with increasing acidity,

these species have rather high distribution coefficients ($\log D > 1$) in the region $0.1 \text{ mol/dm}^3 < [\text{HCl}] < 12 \text{ mol/dm}^3$.⁶ The $\log D$ values of actinide ions increase with increasing acidity, but the values are smaller than 0 for $[\text{HCl}] < 1 \text{ mol/dm}^3$. Therefore, anionic TcO_4^- and other Pt-G elements are considered to be well adsorbed on tertiary pyridine resin and separated from actinides in the same manner as Dowex 1 resin of a weakly basic anion exchanger.

Recovery of RMFP by catalytic electrolytic extraction (Step I-B). Details of the CEE method applied here to Step I-B to recover and purify RMFP obtained from Step 1A were discussed elsewhere.⁷ In principle, Pd^{2+} (or Fe^{2+}) would accelerate electro-deposition of the other ions as a *promoter* (i.e. $\text{Pd}_{\text{adatom}}$) at the electrode surface or as a *mediator* in the bulk solution. As for a typical example of CEE of RMFP from simulated HLLW, the galvanostatic electrolysis resulted in the quantitative deposition, where metal ions with $E^0 > 0.7\text{V}$ tended to deposit on the cathode, and the deposition ratio seemed to be proportional to the order of the redox potential; $\text{Pd} > \text{Te} > \text{Se} > \text{Rh} > \text{Ru} > \text{Re}$. Molybdenum and Zr can be recovered as co-precipitation at $\text{H}^+ < 1.5 \text{ mol/dm}^3$.

An interaction between Pd^{2+} and TcO_4^- during CEE was also confirmed.² The working Pt electrode was polarized from noble to base potential side, every 30 min step by step. The amount of deposition was measured by a radiometric method at each polarized potential. While the deposition of Tc was significantly suppressed with an increase of the nitric acid concentration, addition of Pd^{2+} ($\text{Pd}/\text{Tc} = 5$) enhanced its electro-deposition expectedly even though nitric acid concentration was 2 mol/dm^3 . Namely, the Pd^{2+} effect can conquer a negative nitric acid effect causing the redissolution of Tc deposit. The Tc deposit was brownish in color and apparently not dendritic. The deposition ratio was, however, as low as 2% at maximum, and the deposition amount of Tc was larger than that of Ru under almost the same nitric acid concentration. An observed potential region of TcO_4^- for quantitative electro-deposition was $0.4 \text{ V} - 0.05 \text{ V}$ (V vs. NHE), agreeing with the hydrogen adsorption-desorption potential region of a Pt electrode. The maximum deposition was observed near the hydrogen evolution potential. Thus, H_{ad} likely participates in the electro-deposition of TcO_4^- in the system



In the extremely negative conditions (i.e. $< -0.3\text{V}$), however, hydrogen evolution occurred simultaneously and disturbed again the Tc deposition reaction. In the case of a carbon electrode which had no H_{ad} region in 3 mol/dm^3 nitric acid solution, reduction of TcO_4^- to TcO_2^{2+} was the most significant in the potentiostatic electrolysis at $\phi_E = -0.3 \text{ V}$ or -1.0 V (V vs. Ag/AgCl).⁸

4. Utilization of RMFP

The hydrogen overpotential of metals periodically changes, and specifically Pt-G elements, Re and Tc show lower overpotentials. One can explain those in referring to *d*-hole characteristics based on the band theory. For utilization of RMFP, hydrogen evolution characteristic of the RMFP-deposit on Pt electrodes was investigated for electrolysis in alkaline solution.

RMFP-deposited electrodes were fabricated based on the CEE method. Details of electrolysis conditions are described elsewhere.^{2,9} Results of electrochemical reduction are summarized in Table 2, where "Pd-Ru-Rh-Re (3.5:4:1:1)" means the quaternary Pd-Ru-Rh-Re deposited Pt electrode obtained from electrolyte containing Pd, Ru, Rh and Re (Tc) ions in the ratio of 3.5:4:1:1, which corresponds to the composition of the fast-reactor MOX spent fuel listed in the Table 1. The deposition ratios of RMFP were estimated from the reduction ratios calculated

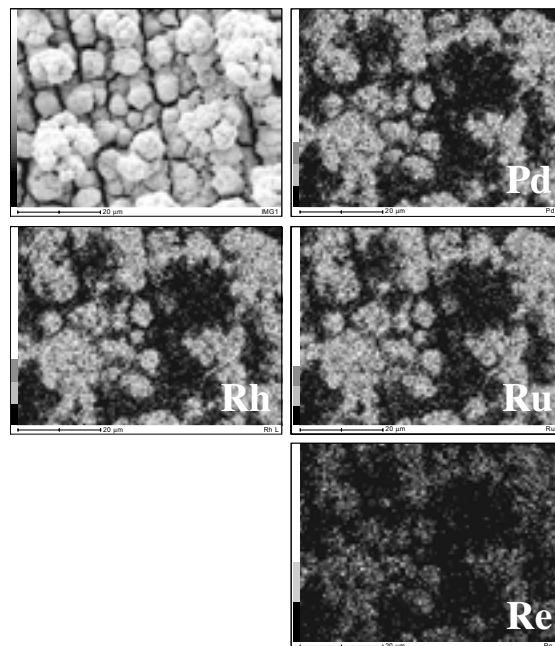


Figure 4. EDS(EPMA) of the deposits on the Pt electrode from nitric acid solution; Solution composition: Pd-Ru-Rh-Re(3.5:4:1:1), divided addition of Pd^{2+} .

from the balance of ionic concentration during the electrolysis. The highest reduction ratio of 95–99% was obtained for Pd by discharging from Pd^{2+} to metallic Pd, and the deposit tended to form dendrites which were easily detached by simultaneous hydrogen evolution. The reduction manner of Rh was similar to that of Pd; a 1 step reduction of Rh^{3+} to metallic Rh. On the contrary, reduction of Ru might proceed by 2 steps, i.e. $\text{RuNO}_3^+ \rightarrow \text{Ru}^{2+}$ and $\text{Ru}^{2+} \rightarrow \text{Ru}$ (metal), with the reduction ratio of around 14%. The reduction ratio was 16% for ReO_4^- and only 1.7% for TcO_4^- . As reported previously,^{1,2,7} the presence of Pd^{2+} accelerated deposition of Rh as well as Ru, and the co-existence of Rh^{3+} also accelerated the reduction of ReO_4^- in the present experiment (16% \rightarrow 43.0%). Specifically, in CEE with a low cathode current density, e.g. 2.5 mA/cm^2 , compulsory stirring was necessary to get a minute and stable deposit of Pd layers. This procedure was very essential to obtain larger amounts of co-deposit with other ions. Figure 4 shows an element map of the surface deposit observed with EPMA (electron probe micro analyzer) for the final run (*2) in Table 2. In this run, Pd^{2+} was added to catholyte divided by 5 times to allow Pd to exist constantly in the bulk solution (as Pd^{2+}) and at the electrode surface (as $\text{Pd}_{\text{adatom}}$). The shape of deposit was not dendritic but rather spherical and homogeneous, likely cohered with fine particles.

TABLE 2: Reduction Ratios of RMFP by Catalytic Electrolytic Extraction

System	Reduction ratio / %					Composition of Electrode Surface
	Pd	Ru	Rh	Re	Tc	
Pd	>99	-	-	-	-	-
Ru	-	14	-	-	-	-
Rh	-	-	>99	-	-	-
Re	-	-	-	16	-	-
Tc	-	-	-	-	1.7	-
Pd-Ru	99.3	60.9	-	-	-	$\text{Pd} \approx \text{Ru}$
Pd-Rh	99.0	-	84.7	-	-	$\text{Pd} \approx \text{Rh}$
Pd-Re	99.4	-	-	10.0	-	$\text{Pd} > \text{Re}$
Ru-Rh	-	58.2	32.5	-	-	$\text{Ru} \approx \text{Rh}$
Ru-Re	-	14.5	-	13.5	-	$\text{Ru} > \text{Re}$
Rh-Re	-	-	10.0	43.0	-	$\text{Rh} > \text{Re}$
Pd-Ru-Rh-Re(1:1:1:1)	95.7	46.0	14.5	19.0	-	$\text{Pd} \approx \text{Ru} \approx \text{Rh} > \text{Re}$
Pd-Ru-Rh-Re(3.5:4:1:1) ^{*1}	99.0	11.8	2.10	33.4	-	$\text{Pd} \approx \text{Ru} \approx \text{Rh} > \text{Re}$
Pd-Ru-Rh-Re(3.5:4:1:1) ^{*2}	94.7	16.5	26.6	55.3	-	$\text{Pd} \approx \text{Ru} \approx \text{Rh} > \text{Re}$

*1: Pd block addition.

*2: Pd 5divided addition.

